


RESEARCH ARTICLE | MAY 13 2025

Phase and gain stability for adaptive dynamical networks



Special Collection: [Advances in Adaptive Dynamical Networks](#)

Nina Kastendiek ; Jakob Niehues  ; Robin Delabays ; Thilo Gross ; Frank Hellmann 



Check for updates

Chaos 35, 053142 (2025)

<https://doi.org/10.1063/5.0249706>



View
Online



Export
Citation

Articles You May Be Interested In

Complexified synchrony

Chaos (May 2024)

Exploring the interplay of excitatory and inhibitory interactions in the Kuramoto model on circle topologies

Chaos (April 2024)

Stability of twisted states on lattices of Kuramoto oscillators

Chaos (October 2021)

Chaos

Special Topics Open
for Submissions

[Learn More](#)

Phase and gain stability for adaptive dynamical networks

Cite as: Chaos 35, 053142 (2025); doi: 10.1063/5.0249706

Submitted: 19 November 2024 · Accepted: 12 March 2025 ·

Published Online: 13 May 2025



View Online



Export Citation



CrossMark

Nina Kastendiek,¹ Jakob Niehues,^{2,3,a)} Robin Delabays,⁴ Thilo Gross,^{1,5,6} and Frank Hellmann²

AFFILIATIONS

¹Institute for Chemistry and Biology of the Marine Environment, University of Oldenburg, 26129 Oldenburg, Germany

²Potsdam Institute for Climate Impact Research (PIK), Member of the Leibniz Association, P.O. Box 60 12 03, D-14412 Potsdam, Germany

³Institut für Mathematik, Technische Universität Berlin, ER 3-2, Hardenbergstrasse 36a, 10623 Berlin, Germany

⁴School of Engineering, University of Applied Sciences of Western Switzerland HES-SO, 1950 Sion, Switzerland

⁵Helmholtz Institute for Functional Marine Biodiversity (HIFMB), 26129 Oldenburg Germany

⁶Alfred Wegener Institute (AWI), Helmholtz Center for Polar and Marine Research, 27570 Bremerhaven, Germany

Note: This paper is part of the Focus Issue on Advances in Adaptive Dynamical Networks.

a) Author to whom correspondence should be addressed: jakob.niehues@pik-potsdam.de

ABSTRACT

In adaptive dynamical networks, the dynamics of the nodes and the edges influence each other. We show that we can treat such systems as a closed feedback loop between edge and node dynamics. Using recent advances on the stability of feedback systems from control theory, we derive local, sufficient conditions for steady states of such systems to be linearly stable. These conditions are local in the sense that they are written entirely in terms of the (linearized) behavior of the edges and nodes. We apply these conditions to the Kuramoto model with inertia written in an adaptive form and the adaptive Kuramoto model. For the former, we recover a classic result, and for the latter, we show that our sufficient conditions match necessary conditions where the latter are available, thus completely settling the question of linear stability in this setting. The method we introduce can be readily applied to a vast class of systems. It enables straightforward evaluation of stability in highly heterogeneous systems.

Published under an exclusive license by AIP Publishing. <https://doi.org/10.1063/5.0249706>

In complex adaptive networks, both the nodes and the connections between them evolve and adapt over time. A fundamental question is, how these evolving interactions influence the system's stability. This paper introduces a new method to analyze such adaptive dynamical systems by treating them as a closed feedback loop between node and edge dynamics. By drawing on recent developments in control theory, we derive a theorem on sufficient conditions for the linear stability of the interconnected system based on the properties of its components. The theorem provides concise local (node-wise and edge-wise) stability conditions. In contrast to standard results, we do not have to assume that all nodes and edges are the same, and our conditions are largely independent of details of the connectivity. We apply these conditions to paradigmatic models in network dynamics and show that they provide new insights and confirm existing results. This approach offers a powerful and accessible tool for evaluating the stability of a wide range of complex systems,

including those with highly heterogeneous components or equilibria.

I. INTRODUCTION

Many systems can be conceptualized as networks in which the network topology is evolving while there are also simultaneously dynamics in the network nodes. If these types of dynamics interact, a feedback loop between local and topological dynamics is formed, and the system can be called an *adaptive network*.¹

Adaptive networks can exhibit rich dynamics and complex self-organization as the network topology evolves dynamically based on past interactions and effectively acts as a memory of previous node dynamics. This increases the dimensionality of the phase space when compared to networks with a fixed topology. Dynamics of adaptive networks play a role in a wide range of phenomena,

including social distancing in epidemics,^{2–4} opinion formation processes in humans^{5–7} and animals,⁸ strategic interactions,^{9,10} neural self-organization,^{11–13} and ecology,¹⁴ among many others.¹⁵

The dynamical interplay between state and topology can result in high-dimensional systems, making mathematical analysis of the dynamics of adaptive networks difficult. Hence, much of the earlier literature in the field focuses on discrete-state adaptive networks that can be modeled by systems of ordinary differential equations using moment expansions.¹⁶ More recently, the master stability function approach^{17,18} has been generalized to broad classes of adaptive networks.^{19,20} However, the use of master stability functions hinges on the symmetry between network nodes. Hence, this approach only allows for stability and bifurcation analysis of homogeneous states of adaptive networks.

In this work, we introduce a new method for analyzing the stability of heterogeneous adaptive dynamical networks by leveraging recent advances in linear algebra and control theory. The key ingredient is to write the system in the form of a feedback loop between node and edge variables, represented by two transfer matrices with a block diagonal structure. Transfer functions model a system's input-output behavior by describing how an input signal is transformed into an output through the dynamics of the system, thus allowing one to understand how a system responds to disturbances.

In feedback systems, the gain of the two transfer functions can be used to give sufficient stability conditions for the interconnected system. The gain of a transfer matrix is well-established and defined in terms of its singular values. It quantifies the largest amplification that a system can provide to an input. However, the gain alone is often insufficient to prove stability.

The central new tool that enables phase analysis in networks is the concept of the phases of a matrix.²¹ It can be regarded as the generalization of the phase of a complex number to linear operators, thus giving information complementary to the gain. It was already observed in Wang *et al.*²² that these phases characterize Laplacians of weighted graphs. The central result of Chen *et al.*²³ is that the phases of transfer matrices can be used to give sufficient stability conditions for higher-dimensional interconnected systems. Zhao *et al.*²⁴ observed that phase and gain information can be combined to cover a much broader class of systems. In this paper, we combine the observation that phase analysis is well-behaved for Laplacian-like systems, with the results of Chen *et al.*²³ and Zhao *et al.*²⁴ to provide novel sufficient stability conditions for adaptive dynamical systems. Furthermore, we leverage the natural block structure of adaptive networks to obtain local instead of global conditions.

We apply these conditions to the paradigmatic adaptive Kuramoto model and find that the sufficient stability condition we provide matches the necessary stability condition of Do *et al.*²⁵ where the latter is applicable. Together, these results completely characterize the stable steady-state configurations of the adaptive Kuramoto model. This demonstrates that, despite their generality, the conditions are not very conservative in this important special case. Furthermore, we recover standard results for the classical Kuramoto model and the Kuramoto model with inertia. A companion paper²⁶ develops the necessary formulations and results to apply these methods to complex oscillator models of power grids.^{27,28}

Our paper proceeds as follows: In Sec. II, we provide an intuitive introduction to the concepts of controlling feedback systems.

In Sec. III A, we recall important fundamental notions in control theory. Readers familiar with control theory can skip these two sections and start with Sec. III B, which gives the central definitions we need for our paper, and Sec. III C, which gives the recent results on the feedback stability of systems that we build upon. In Sec. IV, we give our main results by adapting these concepts to the analysis of adaptive dynamical networks. In Sec. V, we apply them to example systems. We recover state-of-the-art results and extend them to heterogeneous systems.

Throughout the paper, we write capital bold letters for matrices, e.g., \mathbf{M} , and lower case bold letters for vectors, e.g., \mathbf{x} .

II. PHASE STABILITY FOR DYNAMICAL SYSTEMS: A HIGH-LEVEL SKETCH

Here, we give an intuitive introduction to the concepts that we later treat rigorously.

Consider the set of equations,

$$\dot{\mathbf{x}} = -\mathbf{b} \cdot \mathbf{y}, \quad (1)$$

$$\mathbf{y} = \mathbf{d} \cdot \mathbf{x}. \quad (2)$$

These are two systems that are connected by treating the “output” of the one as the “input,” or the driving force of the other.

Such interconnected linear systems are studied in depth in control theory. One system is often considered a “plant,” that is the system we wish to control using the inputs, and the second is a feedback controller. The interconnected system is called the closed-loop system.

One of the foundational results of the theory of the stability of such feedback systems is the small-gain theorem.²⁹ It provides a stability condition in terms of the absolute value of each system's response, an amplification factor called gain: If we drive each of the systems with an oscillation of a fixed frequency, the response will be a phase shifted oscillation with a different amplitude. Assuming $y(t) = e^{i\omega t}$ in the case of (1),

$$\dot{\mathbf{x}} = -\mathbf{b} \cdot \mathbf{y} \quad (3)$$

$$\Rightarrow x(t) = \frac{-\mathbf{b}}{i\omega} e^{i\omega t} + c \quad (4)$$

$$=: \sigma \exp(i\omega t + \phi) + c, \quad (5)$$

where the absolute value $\sigma = \left| \frac{\mathbf{b}}{\omega} \right| > 0$ is called the gain and $\phi = \arg\left(\frac{-\mathbf{b}}{i\omega}\right)$ is called the phase of the response factor $\frac{-\mathbf{b}}{i\omega}$.

The gain at each frequency is (the absolute value of) the factor by which the oscillation at that frequency is amplified or damped. The small-gain theorem²⁹ states that if the product of the gains of the two interconnected systems is smaller than 1 at all frequencies, the interconnected system is stable.

The gain of the second Eq. (2) is just $|d|$; however, the gain of the first equation is $\left| \frac{\mathbf{b}}{\omega} \right|$ and becomes arbitrarily large at $\omega \rightarrow 0$. Consequently, small-gain theorems cannot prove stability of such connected systems.

Allowing \mathbf{b} and \mathbf{d} to be complex, the condition for stability of (1) and (2), which is equivalent to $\dot{\mathbf{x}} = -\mathbf{b}\mathbf{d}\mathbf{x}$, is of course $\Re(\mathbf{b}\mathbf{d}) > 0$.

This result can be recovered by using the phases of the system under study. Small-phase theorems give conditions of the type

$$-\pi < \arg(d) + \arg\left(\frac{b}{i\omega}\right) < \pi. \quad (6)$$

Due to the singularity at $\omega = 0$, the phase condition is evaluated for all $\omega \neq 0$ and $i\omega = \epsilon^+$, where ϵ^+ is a small positive real number approaching zero. The condition then reduces to the exact result $\Re(bd) > 0$. A strong advantage of this condition is that it is invariant under scaling the coefficients b and d by positive values.

The paradigmatic Kuramoto model³⁰ can be written in the same structure as (1) and (2). To linear order, the driving force from the neighboring nodes is provided by a weighted Laplacian multiplying the phases \mathbf{x} . Again, we know linear stability conditions for the simplest case: If the weighted Laplacian \mathbf{L} is positive semi-definite, then $\dot{\mathbf{x}} = -\mathbf{L}\mathbf{x}$ is semi-stable. In particular, this is the case if the weights are positive.

The small-gain theorem was stated for higher-dimensional systems from the start, with the singular values of matrices taking the place of σ above.²⁹ However, in Kuramoto-type models, we typically have that the uncoupled system can move freely along a limit cycle. There is no local force pushing it toward a particular phase, and thus, the gain of the nodal dynamics will often be infinite. Small-gain theorems do not apply for the same reason as in (1) and (2).

In contrast to gain theorems, phase conditions for the stability of higher-dimensional systems were only derived recently.²³ They build on a new definition of the phases of a matrix.²¹ These definitions allow treating systems, such as the linearized Kuramoto oscillator, that are not amenable to small-gain analysis. Intriguingly, the phases ϕ on which these small-phase theorems rely are also invariant under rescaling in the following sense: They are characteristics of a matrix \mathbf{A} that satisfy $\phi(\mathbf{A}) = \phi(\mathbf{M}\mathbf{A}\mathbf{M}^{-1})$ for full rank, square \mathbf{M} .

As we will see, these types of relationships allow us to reduce the phase conditions on the weighted Laplacian \mathbf{L} to phase conditions on the diagonal matrix \mathbf{D} that contains the edge weights. This allows us to get stability conditions independent of the network topology encoded in the node-edge incidence matrix \mathbf{B} since a weighted Laplacian can be written as $\mathbf{L} = \mathbf{B}\mathbf{D}\mathbf{B}^\dagger$. For the simple Kuramoto model, the condition that the weights have to be positive is easily recovered. Thus, the phase analysis subsumes the fact that positive weights imply semi-definite Laplacians.

In the context of phase analysis, the network weights do not need to be constant, though. They can react to the inputs (as mapped to the edges by \mathbf{B}^\dagger), and the phase response of their dynamics will determine the stability characteristics of the full interconnected system.

III. CONTROL THEORY

To make this paper more self-contained for a physics audience, this section reproduces key concepts and results from control theory. We begin by recalling key properties of transfer functions in the one-dimensional case. We then discuss the definition of the magnitude and phase response of higher-dimensional linear systems (in this context typically called multiple-input multiple-output, linear time-invariant: MIMO LTI), and the underlying concepts of the

phases and magnitudes of a matrix. Finally, we present the phase and gain conditions for stability in interconnected feedback systems that we will use below.

A. Transfer functions and stability

Transfer functions are a tool for understanding how linear systems respond to inputs or disturbances, thus providing insights into their behavior and stability. We give an introduction to stability analysis with the help of transfer functions. For more detailed explanations, refer, for example, to Levine³¹ and Bechhoefer.³²

The transfer function of an LTI system relates the system's input to its output in the Laplace domain. The *Laplace transform* converts a function $f(t)$ of a real variable t , typically in the time domain, to a function $F(s)$ of a complex variable s in the complex-valued frequency domain, also called the s -domain,

$$\mathcal{L}\{f(t)\} = F(s) := \int_0^\infty e^{-st} f(t) dt. \quad (7)$$

The complex-valued frequency variable s is defined as $s = \rho + i\omega$, where the real part ρ is related to growth or decay and the imaginary part $i\omega$ corresponds to oscillatory components. Following conventions, we will often use f for the function $f(t)$ and its Laplace transform $F(s)$. The context will make it clear which one is at consideration.

The *transfer function* is defined as the ratio of the Laplace transform of the output $Y(s)$ to the Laplace transform of the input $U(s)$; i.e., $G(s) := \frac{Y(s)}{U(s)}$. It is convention to assume without loss of generality that all initial conditions are zero.

As an example, consider the linear system

$$\dot{x}(t) = -ax(t) + u(t) \quad (8)$$

with initial conditions equal to zero: $x(0) = 0$. Taking the Laplace transform, we have

$$sX(s) = -aX(s) + U(s), \quad (9)$$

$$X(s) = \frac{1}{s+a} U(s). \quad (10)$$

Choosing the state as the output, $y(t) = x(t)$, the transfer function $G(s)$ of the system is

$$\frac{X(s)}{U(s)} = G(s) = \frac{1}{s+a}. \quad (11)$$

Setting the denominator to zero, $s+a=0$ shows that the system has a pole at $s=-a$. The inverse Laplace transform of $G(s)$ is

$$\mathcal{L}^{-1}\left\{\frac{1}{s+a}\right\} = e^{-at}.$$

Since multiplication in the Laplace domain corresponds to convolution in the time domain, the general solution for $x(t)$ follows from $X(s) = G(s)U(s)$ and is given by

$$x(t) = \int_0^t e^{-a(t-t')} u(t') dt', \quad (12)$$

which is the well-known solution of (8) for $x(0) = 0$.

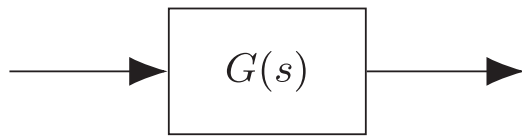


FIG. 1. Open-loop system. Arrows indicate inputs and outputs.

A *real-rational* transfer function can be expressed as $G(s) = \frac{N(s)}{D(s)}$, where $N(s)$ and $D(s)$ are polynomials in s with real coefficients. In a *proper* transfer function, the degree of the numerator polynomial $N(s)$ does not exceed the degree of the denominator polynomial $D(s)$, ensuring that the function does not grow unbounded as $|s|$ approaches infinity. Linearized dynamical systems with real coefficients have real-rational proper transfer functions.

Values of s that satisfy $N(s) = 0$ define the zeros of the system, whereas values of s that satisfy $D(s) = 0$ correspond to the poles of the system.

For a continuous-time LTI system represented by a transfer matrix to be *stable*, all poles must have negative real parts; i.e., they must lie in the left half of the complex plane. In the example above, this corresponds to $a > 0$. This ensures that, for any bounded input, the system's output remains bounded, known as Bounded Input, Bounded Output (BIBO) stability. A system that is *semi-stable* (or marginally stable) can have poles on the imaginary axis, provided no poles exist in the right half of the plane. Any pole with a positive real part indicates instability. The set of *real-rational proper stable* transfer functions is denoted \mathcal{RH}_∞ .

Adding feedback to a system changes the pole locations, which can have stabilizing or destabilizing effects. Even if the open-loop system (see Fig. 1) is stable, feedback can introduce new dynamics that may destabilize the system. A closed-loop system with negative feedback (see Fig. 2) subtracts the feedback signal from the input signal. The transfer function of such a system is given by $T(s) := \frac{G(s)}{1+G(s)}$.

If we add a transfer function $H(s)$ to the feedback path (see Fig. 3), the closed-loop transfer function becomes $T(s) := \frac{G(s)}{1+G(s)H(s)}$. Finding the poles of a closed-loop transfer function is more challenging than for an open-loop system, particularly in systems with multiple inputs and outputs. Instead, the open-loop frequency response $G(s)H(s)$ can be used to determine whether the closed-loop system will be stable. The frequency response evaluates the steady-state behavior of a system by analyzing how it reacts to sinusoidal

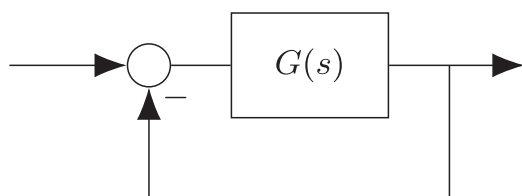


FIG. 2. Closed-loop system. The minus next to the circle indicates the subtraction of external input and output to implement negative feedback.

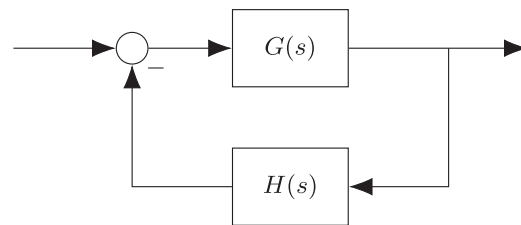


FIG. 3. Closed-loop system with a feedback controller.

inputs across the frequency spectrum $s = i\omega$. When a sine wave is passed through a linear system, the long-term response will also be a sine wave with the same frequency but possibly a different amplitude and phase. Initially, transient effects may occur; however, if the open-loop transfer function is stable (i.e., its poles lie in the stable region), these transients will decay over time, leaving the steady-state response.

The gain of a system, $\sigma(G(i\omega)) := |G(i\omega)|$, describes how the system changes the amplitude of signals at a specific frequency, whereas the phase $\phi(G(i\omega)) := \arg(G(i\omega))$ captures the phase shift introduced by the system to those signals. For real-valued linear time-invariant systems, analyzing the frequency response over $\omega \in [0, \infty]$ is sufficient, as the behavior at negative frequencies is symmetric (magnitude even and phase odd).

The Nyquist criterion gives a condition for the stability of a closed-loop system by analyzing the open-loop transfer function $G(s)H(s)$: Given that $G(s)$ and $H(s)$ have no poles in the right half-plane, the closed-loop system is stable if $1 + G(s)H(s)$ has no zeros in the right half-plane. By integrating along a contour that encloses the right-half plane and applying the Cauchy argument principle, it follows that the number of right-half-plane zeros of $1 + G(s)H(s)$ is equal to the number of counterclockwise encirclements of -1 by the Nyquist plot of $G(s)H(s)$. The Nyquist plot is obtained by plotting the values of $G(j\omega)H(j\omega)$ in the complex plane as ω varies from $-\infty$ to $+\infty$. Thus, if the Nyquist plot of $G(s)H(s)$ does not encircle -1 , then $1 + G(s)H(s)$ can have no zeros in the right half-plane and the closed-loop system is stable. A sufficient condition for no encirclement is that for all frequencies ω , either the gain of $G(i\omega)H(i\omega)$ is smaller than 1 or that the argument does not cross the negative imaginary axis: $-\pi < \arg(G(i\omega)H(i\omega)) < \pi$.

In semi-stable systems with poles on the imaginary axis, the Nyquist contour must be modified to avoid passing through these poles. One approach is to construct a semicircular detour with radius $\epsilon^+ \rightarrow 0$ around imaginary-axis poles into the right-half plane. If the Nyquist plot of $G(s)H(s)$ does not encircle -1 , the closed-loop system is stable.

B. Frequency response of MIMO LTI systems

In multiple-input multiple-output systems, the transfer function is a matrix that describes the relationship between each input and each output. The central challenge in generalizing the arguments above to this case is that we now must give conditions for the eigenvalues of $G(s)H(s)$ to not encircle -1 . While bounding the magnitude of the eigenvalues of $G(s)H(s)$ in terms of the matrix

norms of $\mathbf{G}(s)$ and $\mathbf{H}(s)$ is straightforward, bounding the phases of the eigenvalues in terms of properties of $\mathbf{G}(s)$ and $\mathbf{H}(s)$ is not. This section defines the required vocabulary to state the theorems that we build upon.

1. Gain of a matrix

We begin by introducing the appropriate complex matrix magnitudes and phases, following Chen *et al.*,²³ Zhao *et al.*²⁴ A matrix $\mathbf{M} \in \mathbb{C}^{n \times n}$ has n magnitudes, defined as the n singular values. The *gain* is the maximum singular value and, thus, equal to the spectral norm.

2. Angular numerical range

The *numerical range* of a matrix $\mathbf{M} \in \mathbb{C}^{n \times n}$ is given by

$$W(\mathbf{M}) := \{z^\dagger \mathbf{M} z \mid z \in \mathbb{C}^n, z^\dagger z = 1\}. \quad (13)$$

The numerical range is a compact and convex subset of \mathbb{C} and contains the spectrum of \mathbf{M} . The *angular numerical range* of \mathbf{M} is defined as

$$W'(\mathbf{M}) := \{z^\dagger \mathbf{M} z \mid z \in \mathbb{C}^n, z^\dagger z > 0\}, \quad (14)$$

which is the conic hull of $W(\mathbf{M})$ and is always a convex cone (or the entire complex plane).

3. Sectorial matrices and their sector

If 0 is not in $W(\mathbf{M})$, the matrix is *sectorial*. If 0 is on the boundary of $W(\mathbf{M})$, it is *semi-sectorial*. For a semi-sectorial matrix that is not identical to zero, $\arg(W'(\mathbf{M}))$ defines a sector of the circle of length $2\Delta(\mathbf{M}) \leq \pi$. The phase for the midpoint of this sector is only defined modulo 2π , and we typically choose the phase of the midpoint $\gamma(\mathbf{M})$ such that $-\pi \leq \gamma(\mathbf{M}) \leq \pi$. The maximum and minimum phase of \mathbf{M} are then defined as $\bar{\phi}(\mathbf{M}) := \gamma(\mathbf{M}) + \Delta(\mathbf{M})$ and $\underline{\phi}(\mathbf{M}) := \gamma(\mathbf{M}) - \Delta(\mathbf{M})$. Note that this means that $\bar{\phi}(\underline{\phi})$ can be larger (smaller) than π ($-\pi$).

4. Stable frequency-wise sectorial transfer matrices

A system $\mathbf{G} \in \mathcal{RH}_\infty^{m \times m}$ is said to be *frequency-wise sectorial* if $\mathbf{G}(i\omega)$ is sectorial for all $\omega \in [-\infty, \infty]$.

5. Semi-stable frequency-wise semi-sectorial transfer matrices

Let \mathbf{G} be an $m \times m$ real-rational proper semi-stable system with no poles in the open right half-plane and $i\Omega$ the set of poles on the imaginary axis. \mathbf{G} is *frequency-wise semi-sectorial* if

1. $\mathbf{G}(i\omega)$ is semi-sectorial for all $\omega \in [-\infty, \infty] \setminus \Omega$ and
2. there exists an $\epsilon^* > 0$ such that for all $\epsilon^+ \leq \epsilon^*$, $\mathbf{G}(s)$ has a constant rank and is semi-sectorial along the indented imaginary axis, where the half-circle detours to the right with radius ϵ^+ are taken around both the poles and finite zeros of $\mathbf{G}(s)$ on the frequency axis and a half-circle detour with radius $1/\epsilon^+$ is taken if infinity is a zero of $\mathbf{G}(s)$.

Analogous definitions hold for stable frequency-wise semi-sectorial and semi-stable frequency-wise sectorial systems.

6. Frequency-wise gain response of a system

With these definitions, we can now introduce the magnitude and phase response of MIMO LTI systems, following Chen *et al.*,²³ Zhao *et al.*²⁴ Let \mathbf{G} be an $m \times m$ real-rational proper transfer matrix. Then, $\sigma(\mathbf{G}(i\omega))$ is the vector of singular values of $\mathbf{G}(i\omega)$, which is called the magnitude response of \mathbf{G} . The gain at frequency ω is the largest singular value $\bar{\sigma}(\mathbf{G}(i\omega))$.

7. Frequency-wise phase response of a system

Consider a frequency-wise sectorial (semi-sectorial) system $\mathbf{G}(s)$. At zero frequency, $\mathbf{G}(0)$ (or $\mathbf{G}(\epsilon^+)$) is real. For a real matrix, the angular field of values is symmetric with respect to the real axis. Thus, for a sectorial (semi-sectorial) system, the phase center $\gamma(\mathbf{G}(0))$ [or $\gamma(\mathbf{G}(\epsilon^+))$] is either 0 or π (modulo 2π). The phase center at zero frequency is referred to as the DC phase center.³³ We require that the phase center of $\mathbf{G}(0)$ [or $\mathbf{G}(\epsilon^+)$] can be chosen as 0. In the context of feedback, this means using the freedom to assign roots of 1 to the two transfer matrices without loss of generality. This enables a practical representation that avoids the critical point and the branch cut at π and $-\pi$. We choose phase centers for $\mathbf{G}(i\omega)$ such that $\gamma(\mathbf{G}(i\omega))$ is continuous in the frequency $\omega \in [-\infty, \infty]$ (or on the contour avoiding the poles). Then, $[\bar{\phi}(\mathbf{G}(i\omega)), \underline{\phi}(\mathbf{G}(i\omega))]$ is the sector containing the phase response of $\mathbf{G}(s)$.

Note that the gain response is an even, the phase response is an odd function of the frequency ω . Small-gain and phase theorems of real-valued systems are often given in terms of conditions for only $\omega \in [0, \infty]$.

C. Feedback stability in MIMO LTI systems

We can now state the main theorems we will adapt to the adaptive network context below.

Denote the identity matrix \mathbf{I} . The feedback system in Fig. 4, denoted $\mathbf{G}\#\mathbf{H}$, is stable if the Gang of Four matrix

$$\mathbf{G}\#\mathbf{H} := \begin{bmatrix} (\mathbf{I} + \mathbf{H}\mathbf{G})^{-1} & (\mathbf{I} + \mathbf{H}\mathbf{G})^{-1}\mathbf{H} \\ \mathbf{G}(\mathbf{I} + \mathbf{H}\mathbf{G})^{-1} & \mathbf{G}(\mathbf{I} + \mathbf{H}\mathbf{G})^{-1}\mathbf{H} \end{bmatrix} \quad (15)$$

is stable; i.e., $\mathbf{G}\#\mathbf{H} \in \mathcal{RH}_\infty$. $\mathbf{G}\#\mathbf{H}$ relates all inputs and outputs of the interconnected feedback loop.

To obtain stability conditions, we need to make sure that $\mathbf{I} + \mathbf{H}(s)\mathbf{G}(s)$ has no zero eigenvalues on the right-hand side of the complex plane. This can be achieved by limiting either the gain^{29,34} or the phase²³ response of \mathbf{G} and \mathbf{H} .

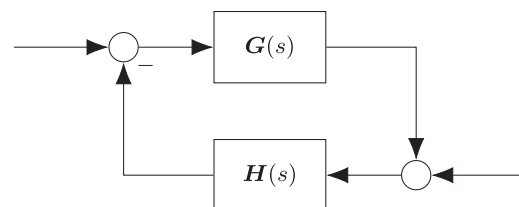


FIG. 4. Feedback system.

Theorem 1 (Small-gain theorem, Zames,²⁹ and Zhou³⁴): Let \mathbf{G} and $\mathbf{H} \in \mathcal{RH}_{\infty}^{n \times n}$. Then, the feedback system $\mathbf{G}\#\mathbf{H}$ is stable if

$$\bar{\sigma}[\mathbf{G}(i\omega)]\bar{\sigma}[\mathbf{H}(i\omega)] < 1 \quad (16)$$

for all $\omega \in [-\infty, \infty]$.

Theorem 2 (Generalized small-phase theorem, Chen *et al.*²³): Let \mathbf{G} be semi-stable frequency-wise semi-sectorial with $i\Omega$ being the set of poles on the imaginary axis and $\mathbf{H} \in \mathcal{RH}_{\infty}^{n \times n}$ be frequency-wise sectorial. Then, $\mathbf{G}\#\mathbf{H}$ is stable if

$$\bar{\phi}(\mathbf{G}(i\omega)) + \bar{\phi}(\mathbf{H}(i\omega)) < \pi, \quad (17)$$

$$\underline{\phi}(\mathbf{G}(i\omega)) + \underline{\phi}(\mathbf{H}(i\omega)) > -\pi \quad (18)$$

for all $\omega \in [0, \infty] \setminus \Omega$.

Both conditions can be combined. The mixed gain-phase theorem with cut-off frequency developed by Zhao *et al.*²⁴ provides stability results for feedback systems that satisfy a phase condition at low frequencies and a gain condition at high frequencies.

Theorem 3 (Mixed gain-phase theorem with cut-off frequency, Zhao *et al.*²⁴): Let $\omega_c \in (0, \infty)$, \mathbf{G} be semi-stable frequency-wise semi-sectorial over $(-\omega_c, \omega_c)$ with $i\Omega$ being the set of poles on the imaginary axis satisfying $\max_{\omega \in \Omega} |\omega| < \omega_c$ and $\mathbf{H} \in \mathcal{RH}_{\infty}^{n \times n}$ be frequency-wise sectorial. Then, $\mathbf{G}\#\mathbf{H}$ is stable if

(i) for each $\omega \in [0, \omega_c) \setminus \Omega$, it holds

$$\bar{\phi}(\mathbf{G}(i\omega)) + \bar{\phi}(\mathbf{H}(i\omega)) < \pi, \quad (19)$$

$$\underline{\phi}(\mathbf{G}(i\omega)) + \underline{\phi}(\mathbf{H}(i\omega)) > -\pi, \quad (20)$$

(ii) and for each $\omega \in [\omega_c, \infty]$, it holds

$$\bar{\sigma}(\mathbf{G}(i\omega))\bar{\sigma}(\mathbf{H}(i\omega)) < 1. \quad (21)$$

Woolcock and Schmid³⁵ give a further generalized version and a proof that proceeds by the Nyquist criterion but does not treat the semi-stable case, which we need in the following.

IV. STABILITY OF ADAPTIVE NETWORKS

We now come to the main result of the paper: An adaptation of the mixed gain-phase condition to the case of adaptive dynamical networks.

We will first show in detail how such systems can be written as interconnected feedback systems. Then, we will give the main theorems.

A. Adaptive networks as feedback systems

In this section, we show that a broad class of adaptive dynamical systems can be cast into the form of a feedback system. In the neighborhood of a steady state, the subsystems in the feedback loop are represented by two transfer matrices.

Let the N nodes of the network be indexed n and m , with $1 \leq n, m \leq N$. The L edges are indexed by ordered pairs $l = (n, m)$, $n < m$. For any nodal quantity \mathbf{x}_n^v , we denote \mathbf{x}^v the overall vector obtained by stacking the \mathbf{x}_n^v , similarly for \mathbf{x}_l^e . Note that, unless otherwise stated, the dimension of \mathbf{x}_l^e and \mathbf{x}_n^v can vary from edge to edge and node to node.

Consider a general bipartite dynamical system associated with a graph with node variables \mathbf{x}^v and edge variables \mathbf{x}^e . As noted, the nodes and edges can be heterogeneous; e.g., the states \mathbf{x}_1^v at node 1 can be a vector of a different size and follow different dynamics than \mathbf{x}_2^v at node 2. However, we require that the coupling on the network occurs with respect to some observables \mathbf{o}^v and \mathbf{o}^e that have the same dimension for all edges and nodes. The nodes and edges of the system are coupled with their respective inputs and outputs by a node-edge incidence matrix \mathbf{B} that encodes the graph structure,

$$\dot{\mathbf{x}}^v = \mathbf{f}^v(\mathbf{x}^v, \mathbf{B}\mathbf{o}^e), \quad (22)$$

$$\mathbf{o}^v := \mathbf{g}^v(\mathbf{x}^v, \mathbf{B}\mathbf{o}^e), \quad (23)$$

$$\dot{\mathbf{x}}^e = \mathbf{f}^e(\mathbf{x}^e, \mathbf{B}^\dagger \mathbf{o}^v), \quad (24)$$

$$\mathbf{o}^e := \mathbf{g}^e(\mathbf{x}^e, \mathbf{B}^\dagger \mathbf{o}^v), \quad (25)$$

where \mathbf{f} and \mathbf{g} act node-wise or edge-wise, that is,

$$\dot{\mathbf{x}}_n^v = \mathbf{f}_n^v(\mathbf{x}_n^v, \mathbf{B}\mathbf{o}^e|_n) \quad \text{etc.} \quad (26)$$

With $\mathbf{o}^e := \mathbf{B}\mathbf{o}^e$, we have

$$\dot{\mathbf{x}}^v = \mathbf{f}^v(\mathbf{x}^v, \mathbf{o}^e), \quad (27)$$

$$\mathbf{o}^v := \mathbf{g}^v(\mathbf{x}^v, \mathbf{o}^e), \quad (28)$$

$$\dot{\mathbf{x}}^e = \mathbf{f}^e(\mathbf{x}^e, \mathbf{B}^\dagger \mathbf{o}^v), \quad (29)$$

$$\mathbf{o}^e := \mathbf{B}\mathbf{g}^e(\mathbf{x}^e, \mathbf{B}^\dagger \mathbf{o}^v). \quad (30)$$

Here, each component of \mathbf{f}^v and \mathbf{f}^e contains the local dynamics of \mathbf{x}_n^v and \mathbf{x}_l^e and also the coupling to the output of the other half of the bipartite system. Similarly, each component of \mathbf{g}^v and \mathbf{g}^e contains the local output functions of \mathbf{x}_n^v and \mathbf{x}_l^e . Without loss of generality, we assume that the fixed point we want to study is at the origin $\mathbf{x}^* = 0$. The linearized system has the form

$$\dot{\mathbf{x}}^v = \mathbf{J}^{vv}\mathbf{x}^v + \mathbf{J}^{ve}\mathbf{o}^e, \quad (31)$$

$$\mathbf{o}^v := \mathbf{D}^{vv}\mathbf{x}^v + \mathbf{D}^{ve}\mathbf{o}^e, \quad (32)$$

$$\dot{\mathbf{x}}^e = \mathbf{J}^{ee}\mathbf{x}^e + \mathbf{J}^{ev}\mathbf{B}^\dagger \mathbf{o}^v, \quad (33)$$

$$\mathbf{o}^e := \mathbf{B}\mathbf{D}^{ee}\mathbf{x}^e + \mathbf{B}\mathbf{D}^{ev}\mathbf{B}^\dagger \mathbf{o}^v. \quad (34)$$

The Jacobians (or *system matrices*) \mathbf{J}^{vv} and \mathbf{J}^{ee} capture the intrinsic dynamics of the node and edge states, while the *input matrices* \mathbf{J}^{ve} and \mathbf{J}^{ev} describe how the inputs from the other half of the bipartite system affect these states. The *output matrices* \mathbf{D}^{vv} and \mathbf{D}^{ee} define how the states contribute to their respective outputs, and the *feedthrough matrices* \mathbf{D}^{ve} and \mathbf{D}^{ev} represent the direct influence of inputs on outputs. In the most common notions of adaptive networks, we have $\mathbf{D}^{ve} = \mathbf{0}$. Otherwise, this system might correspond to a differential algebraic equation, rather than a differential equation.

As the dynamics of \mathbf{f} and \mathbf{g} act locally at the nodes, the matrices $\mathbf{J}^{\bullet\bullet}$ and $\mathbf{D}^{\bullet\bullet}$ are block diagonal,

$$\mathbf{J}^{\bullet\bullet} = \bigoplus_n \mathbf{J}^{\bullet\bullet}_n, \quad \mathbf{J}^{\bullet\bullet} = \bigoplus_l \mathbf{J}^{\bullet\bullet}_l \quad (35)$$

and for the $\mathbf{D}^{\bullet\bullet}$ accordingly. \bigoplus denotes the direct sum over nodes or edges.

We now go to Laplace space³⁶ and obtain the transfer matrices of the system: Time derivatives are replaced by a factor s , and we can algebraically solve (31)–(34) for the outputs in terms of the inputs,

$$\mathbf{o}^v = (\mathbf{D}^{vv}(s) - \mathbf{J}^{vv})^{-1} \mathbf{J}^{ve} + \mathbf{D}^{ve}) \mathbf{o}^e \quad (36)$$

$$:= \mathbf{T}^{ve}(s) \mathbf{o}^e \quad (37)$$

$$\mathbf{o}^e = \mathbf{B} (\mathbf{D}^{ee}(s) - \mathbf{J}^{ee})^{-1} \mathbf{J}^{ev} + \mathbf{D}^{ev}) \mathbf{B}^\dagger \mathbf{o}^v \quad (38)$$

$$:= -\mathbf{B} \mathbf{T}^{ev}(s) \mathbf{B}^\dagger \mathbf{o}^v. \quad (39)$$

If \mathbf{B}^\dagger has a kernel, there are directions in phase space that are not visible to the network interactions since there exist vectors in the node space that get mapped to zero when projected onto the edge space by \mathbf{B}^\dagger . Note that in this situation, the stability results are with respect to outputs that are orthogonal to this zero mode.

The inner transfer matrices of these systems are block diagonal: they can be written as the direct sum of node-wise or edge-wise transfer matrices,

$$\mathbf{T}^{ve} = \bigoplus_n \mathbf{T}^{ve}_n, \quad \mathbf{T}^{ev} = \bigoplus_l \mathbf{T}^{ev}_l. \quad (40)$$

The total system is then given by $\mathbf{G}\#\mathbf{H}$ with

$$\mathbf{H} = \mathbf{T}^{ve}, \quad \mathbf{G} = \mathbf{B} \mathbf{T}^{ev} \mathbf{B}^\dagger. \quad (41)$$

The structure is shown in Fig. 5. One sees immediately that this system class has the proper form to apply Theorem 3. In conclusion, phase and gain can be used to study the linear stability of fixed points in any dynamical system of the general form given in (22)–(25). This includes adaptive networks with nonlinear, heterogenous dynamics. However, Theorem 3 so far only gives us global conditions. In the following, we derive a version that leverages the block structure to provide local conditions.

B. Phases and gains for networked systems

The proofs we give below rely on the lemmas presented in a companion paper.²⁶ Here, we collect the crucial properties of the phases and the gain that make them particularly useful for studying systems with a network structure encoded in an incidence-like matrix \mathbf{B} .

1. Connectivity does not enlarge the phase response

The angular field of values of the transformed matrix $\mathbf{B} \mathbf{M} \mathbf{B}^\dagger$ is contained within the union of the angular field of values of the

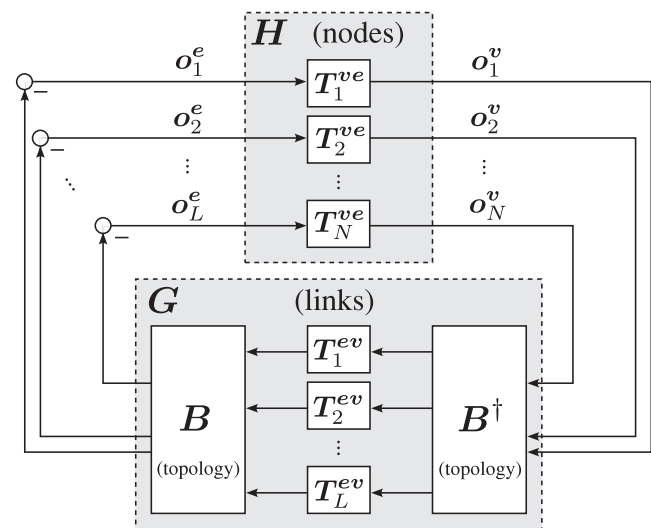


FIG. 5. Block diagram of an adaptive network, linearized and written as a feedback system.

matrix \mathbf{M} with 0,

$$W'(\mathbf{B} \mathbf{M} \mathbf{B}^\dagger) \subseteq (W'(\mathbf{M}) \cup 0), \quad (42)$$

and thus, the phase sector of $\mathbf{B} \mathbf{M} \mathbf{B}^\dagger$ is contained in that of \mathbf{M} ,

$$\bar{\phi}(\mathbf{B} \mathbf{M} \mathbf{B}^\dagger) \leq \bar{\phi}(\mathbf{M}), \quad \underline{\phi}(\mathbf{B} \mathbf{M} \mathbf{B}^\dagger) \geq \underline{\phi}(\mathbf{M}). \quad (43)$$

2. Composition does not enlarge the phase response

For a block diagonal system $\mathbf{T} = \bigoplus_n \mathbf{T}_n$, the numerical range is the convex hull of the numerical ranges of the blocks,

$$W(\mathbf{T}) = \text{Conv}(W(\mathbf{T}_1), \dots, W(\mathbf{T}_N)). \quad (44)$$

Therefore,

$$\bar{\phi}(\mathbf{T}) = \max_n \bar{\phi}(\mathbf{T}_n), \quad \underline{\phi}(\mathbf{T}) = \min_n \underline{\phi}(\mathbf{T}_n) \quad (45)$$

if \mathbf{T} is (semi-)sectorial.

3. The gain increase from connectivity is bounded

The spectral norm is submultiplicative,³⁷ so we can give an upper bound for the spectral norm of the transformed matrix $\mathbf{B} \mathbf{M} \mathbf{B}^\dagger$,

$$\bar{\sigma}(\mathbf{B} \mathbf{M} \mathbf{B}^\dagger) \leq \bar{\sigma}(\mathbf{B}^\dagger) \bar{\sigma}(\mathbf{B}) \bar{\sigma}(\mathbf{M}) = \bar{\sigma}(\mathbf{B})^2 \bar{\sigma}(\mathbf{M}). \quad (46)$$

Defining the unweighted Laplacian matrix \mathbf{L} of the interconnection matrix \mathbf{B} by $\mathbf{L} = \mathbf{B} \mathbf{B}^\dagger$ and noting that $\bar{\sigma}(\mathbf{B})^2 = \bar{\sigma}(\mathbf{L})$, we get

$$\bar{\sigma}(\mathbf{B} \mathbf{M} \mathbf{B}^\dagger) \leq \bar{\sigma}(\mathbf{L}) \bar{\sigma}(\mathbf{M}). \quad (47)$$

Note that the largest singular value of the Laplacian $\bar{\sigma}(\mathbf{L})$ is bounded by twice the maximal degree.

4. Composition does not increase the gain

The spectral norm of a block diagonal system $T = \bigoplus_i T_i$ is the maximum of the spectral norms of its blocks,

$$\bar{\sigma}(T) = \max_i \bar{\sigma}(T_i). \quad (48)$$

C. Small phase and small gain for stability in adaptive networks

We are now ready to give the main results of this paper, a theorem that guarantees the stability of adaptive dynamical systems using gain and phase information. This generalizes the small-phase theorem with block structure given in the companion paper.²⁶

Theorem 4 (Generalized small-phase theorem with block structure²⁶): Consider the system $G\#H$ with the block structure $H = \bigoplus_{n=1}^N T_n(s)$ and $G = B \bigoplus_{l=1}^L T_l(s) B^\dagger$ for some B of appropriate dimensions. For each n , let $T_n(s) \in \mathcal{RH}_\infty$ be frequency-wise sectorial. For each l , let $T_l(s)$ be semi-stable frequency-wise semi-sectorial, with $i\Omega$ being the union of the set of poles on the imaginary axis. Require that $G(s)$ has a constant rank on the indented imaginary axis. Then, the interconnected system $G\#H$ is stable if

$$\max_n \bar{\phi}(T_n(i\omega)) - \min_n \underline{\phi}(T_n(i\omega)) < \pi, \quad (49)$$

$$\max_l \bar{\phi}(T_l(i\omega)) - \min_l \underline{\phi}(T_l(i\omega)) \leq \pi \quad (50)$$

for all $\omega \notin \Omega$, and

$$\sup_{n,l,\omega \notin \Omega} [\bar{\phi}(T_n(i\omega)) + \bar{\phi}(T_l(i\omega))] < \pi, \quad (51)$$

$$\inf_{n,l,\omega \notin \Omega} [\underline{\phi}(T_n(i\omega)) + \underline{\phi}(T_l(i\omega))] > -\pi. \quad (52)$$

We now proceed to our main result. In the Kuramoto model with inertia, for example, the gain becomes arbitrarily large at low frequencies and the phase approaches $-\pi$ at high frequencies. Consequently, neither the small-gain theorem nor the small-phase theorem can prove stability. The mixed small-gain small-phase theorem provides a more flexible and less conservative stability condition for systems with a low phase at small frequencies and a small gain at high frequencies. In analogy to Theorem 3, we can prove a mixed theorem for systems with a block structure.

Proposition 1 (Mixed gain-phase theorem with a cut-off frequency and a block structure): Consider the system $G\#H$ with the block structure $H = \bigoplus_{n=1}^N T_n(s)$ and $G = B \bigoplus_{l=1}^L T_l(s) B^\dagger$ for some B of appropriate dimensions. Let $\omega_c \in (0, \infty)$. For each n , let $T_n(s) \in \mathcal{RH}_\infty$ be frequency-wise sectorial. For each l , let $T_l(s)$ be semi-stable frequency-wise semi-sectorial over $(-\omega_c, \omega_c)$, with $i\Omega$ being the union of the set of poles on the imaginary axis satisfying $\max_{\omega \in \Omega} |\omega| < \omega_c$. Consider that $T_l(s)$ has full rank along the indented imaginary axis. Then, the interconnected system $G\#H$ is stable if

$$\max_n \bar{\phi}(T_n(i\omega)) - \min_n \underline{\phi}(T_n(i\omega)) < \pi \quad (53)$$

for all $\omega \notin \Omega$ and

$$\max_l \bar{\phi}(T_l(i\omega)) - \min_l \underline{\phi}(T_l(i\omega)) < \pi \quad (54)$$

for $\omega \in (-\omega_c, \omega_c) \setminus \Omega$, and

(i) for each $\omega \in [0, \omega_c) \setminus \Omega$, it holds

$$\sup_{n,l} [\bar{\phi}(T_n(i\omega)) + \bar{\phi}(T_l(i\omega))] < \pi, \quad (55)$$

$$\inf_{n,l} [\underline{\phi}(T_n(i\omega)) + \underline{\phi}(T_l(i\omega))] > -\pi. \quad (56)$$

(ii) For each $\omega \in [\omega_c, \infty)$, it holds

$$\sup_{n,l} [\bar{\sigma}(B)^2 \bar{\sigma}(T_n(i\omega)) \bar{\sigma}(T_l(i\omega))] < 1. \quad (57)$$

Remark 1: H is stable, and its sectoriality is ensured by (53). G is semi-stable, and its semi-sectoriality over $(-\omega_c, \omega_c)$ is ensured by (54). Note that the full rank condition, together with semi-sectoriality, implies that each $T_l(s)$ is actually sectorial; thus, (54) has a $<$ instead of \leq in (50). Due to the kernel of B^\dagger , G will still only be semi-sectorial. The DC phase center of both H and G must be 0; i.e., $H(0) = 0$ and $G(\epsilon^+) = 0$. Equations (55)–(56) imply the phase conditions (19) and (20) of Theorem 3, and (57) implies the gain condition (21).

Proof. The proof relies on lemmas of Niehues *et al.*²⁶ and Lemma 6 in the Appendix. Here, it is shown that all assumptions and conditions allow us to apply Theorem 3.

1. Stability of H (Lemma 8²⁶)

If each block $T_n(s)$ is stable, then $H(s) = \bigoplus_{n=1}^N T_n(s)$ is also stable, because the set of its poles is the union of the poles of the blocks.

2. Sectoriality of H (Lemma 9²⁶)

Due to (44), we have that $W(H)$ is the convex hull of all $W(T_n)$. Therefore, if the blocks $T_n(s)$ are frequency-wise sectorial and the phase condition (53) is satisfied, $W(H)$ is contained in a sector of angle $\delta(H) < \pi$. Furthermore, as none of the $W(T_n)$ contains the origin, $W(H)$ does not contain the origin. Since the above holds for any $s \in i[0, \infty]$, we conclude that $H(s)$ is frequency-wise sectorial.

3. Semi-stability of G (Lemma 10²⁶)

Suppose each block $T_l(s)$ is semi-stable and the matrix B is independent of s , i.e., it does not introduce any new poles. Then, $G(s) = B \bigoplus_{l=1}^L T_l(s) B^\dagger$ is semi-stable, because the poles of $G(s)$ are a subset of the union of the poles of the blocks.

4. Constant rank of G (Lemma 6 in the Appendix)

A semi-stable frequency-wise semi-sectorial system must have a constant rank along the indented imaginary axis. If B^\dagger has a kernel, certain directions in $\bigoplus_{l=1}^L T_l(s)$ are projected to zero by B^\dagger . If $\bigoplus_{l=1}^L T_l(s)$ is rank-deficient, its kernel may interact with the kernel of B^\dagger , potentially varying the rank of $G(s)$ across frequencies. We can ensure constant rank of $G(s)$ by requiring $\bigoplus_{l=1}^L T_l(s)$, and thus, each $T_l(s)$, to be full rank for all s . This guarantees that $\ker(G(s)) = \ker(B^\dagger)$ and $G(s)$ has a constant rank along the indented imaginary axis.

5. Semi-sectoriality of G (Lemma 11²⁶)

First, the full rank condition, together with the semi-sectoriality of the blocks $T_l(s)$ over $(-\omega_c, \omega_c)$, implies that the blocks are actually frequency-wise sectorial since 0 cannot be in their numerical range. If the phase condition (54) holds for all blocks, then $\bigoplus_{l=1}^L T_l(s)$ is frequency-wise sectorial over $(-\omega_c, \omega_c)$ by the convex hull property (44). From the subset property (42), we see that the transformation $B \bigoplus_{l=1}^L T_l(s) B^\dagger$ does not enlarge the phase response. However, due to the kernel of B^\dagger , the numerical range $W(G)$ includes 0. Thus, we conclude that $G(s)$ is frequency-wise semi-sectorial over $(-\omega_c, \omega_c)$.

6. Phase condition

Using the convex hull property (44), in particular, (45), and the subset property (42), the assumptions (55) and (56) imply that for each $\omega \in [0, \omega_c) \setminus \Omega$, it holds

$$\bar{\phi} \left(\bigoplus_n T_n(i\omega) \right) + \bar{\phi} \left(B \bigoplus_l T_l(i\omega) B^\dagger \right) < \pi, \quad (58)$$

$$\underline{\phi} \left(\bigoplus_n T_n(i\omega) \right) + \underline{\phi} \left(B \bigoplus_l T_l(i\omega) B^\dagger \right) > -\pi, \quad (59)$$

which are the phase conditions (19) and (20) of Theorem 3.

7. Gain condition

By the submultiplicative property (46) and the spectral norm property (48) and (57) implies that for each $\omega \in [\omega_c, \infty]$, it holds

$$\bar{\sigma} \left(\bigoplus_n T_n(i\omega) \right) \bar{\sigma} \left(B \bigoplus_l T_l(i\omega) B^\dagger \right) < 1, \quad (60)$$

which is the gain condition (21) of Theorem 3.

All in all, the system $(\bigoplus_n T_n) \# (B \bigoplus_l T_l B^\dagger)$ then satisfies all assumptions and conditions of Theorem 3 and is, therefore, stable, which concludes the proof. \square

V. STABILITY OF KURAMOTO-TYPE ADAPTIVE SYSTEMS

We now use Theorem 4 and Proposition 5 to derive sufficient criteria for the stability of several Kuramoto-type systems. We demonstrate that this theorem can give novel insights, even for well studied paradigmatic models.

The first example is the classical Kuramoto model. We recover standard results and show that our theorem includes heterogeneous parameters and complex topologies, as well as complexified states and parameters. The second example is the reformulation of the Kuramoto model with inertia as an adaptive system. Here, we recover established sufficient stability conditions in a novel way. The third system is a proper adaptive Kuramoto model. Here, we obtain new sufficient stability conditions that match the necessary conditions of Do *et al.*²⁵ but also generalize to heterogeneous parameters.

We write $[x]$ for the diagonal matrix with the entries of x on the diagonal.

A. The classical Kuramoto model and its generalizations

Our results also apply to the subclass of non-adaptive systems. Picking up the motivating example of II, consider the classical Kuramoto model³⁰ of N oscillators with phases x_n and natural frequencies f_n , but allow a complex network topology and heterogeneous symmetric coupling weights K_{nm} ,

$$\dot{x}_n = f_n - \sum_m K_{nm} \sin(x_n - x_m). \quad (61)$$

In the steady state x_n° , all oscillators oscillate with a common frequency $\dot{x}_n^\circ = \Omega_{\text{sync}} = \frac{1}{N} \sum_n f_n$, where $f_n = \sum_m K_{nm} \sin(x_n^\circ - x_m^\circ)$. Without loss of generality, we assume $\sum_n f_n = 0$.

The network structure can be represented in an $N \times L$ signed incidence matrix B , with all edges oriented from node n to node m ; i.e., $l = (n, m)$ with $n < m$. The entries of the matrix indicate how the edges connect to the nodes: a value of +1 indicates that the edge is directed away from a node, -1 indicates that the edge is directed toward a node, and 0 means that the node is not connected to that edge.

We linearize the system around the phase-locked state and introduce the error coordinates $\Delta x := x - x^\circ$, and with $x := (x_1, x_2, \dots, x_N)^\top$ and $K := \text{diag}(K_1, K_2, \dots, K_L)$, we get

$$\Delta \dot{x} = -\frac{1}{s} BK [\cos(B^\top x^\circ)] B^\top \Delta x, \quad (62)$$

where $BK [\cos(B^\top x^\circ)] B^\top$ is the weighted Laplacian of the system. The feedback system can be represented by $I \# BD(s) B^\top$, where $D(s) = \frac{1}{s} K [\cos(B^\top x^\circ)]$ is a diagonal matrix. The identity matrix is stable and frequency-wise sectorial with a DC phase center of 0. The operator $D(s)$ has a pole on the imaginary axis at $s = 0$ and is, therefore, semi-stable. Moreover, $D(s)$ must be frequency-wise semi-sectorial and full rank with the DC phase center $D(\epsilon^+) = 0$. It follows that $K_{nm} \cos(x_n^\circ - x_m^\circ) > 0$ for all edges $l = (n, m)$. With this, the phase condition

$$-\pi < \arg(1) + \arg\left(\frac{1}{i\omega} K_{nm} \cos(x_n^\circ - x_m^\circ)\right) < \pi \quad (63)$$

is fulfilled for all $\omega \in (0, \infty]$, and we can prove stability according to Theorem 4. The stability condition $K_{nm} \cos(x_n^\circ - x_m^\circ) > 0$ implies phase differences $|x_n^\circ - x_m^\circ| < \pi/2$ for all edges $l = (n, m)$, a classical result that we here get straightforward. A key advantage of applying Theorem 4 is that we can immediately analyze the diagonal matrix D and the network structure in B drops out.

Furthermore, our method almost immediately applies³⁸ to the complexified Kuramoto model introduced by Thümler *et al.*,³⁹ Lee *et al.*⁴⁰ It follows the same dynamics (61) as the classical Kuramoto model, but the state and parameters are continued to the complex plane. This complexified system is stable if all $\Re(K_{nm} \cos x_n^\circ - x_m^\circ) > 0$ for all connected (n, m) .

B. The Kuramoto model with inertia

As a first detailed example, we study the Kuramoto model with inertia^{41,42} in the most general case of heterogeneous parameters,

$$m_n \ddot{x}_n + \gamma_n \dot{x}_n = P_n - \sum_m K_{nm} \sin(x_n - x_m), \quad (64)$$

where x_n represents the phase of the n th oscillator with inertia $m_n > 0$, torque P_n , and damping γ_n . K_{nm} is the coupling strength of the edge connecting n and m , with $K_{nm} = 0$ if there is no edge.

By introducing the dynamic coupling variable κ_{nm} , (64) can be rewritten as a system of N adaptively coupled phase oscillators,

$$m_n \dot{x}_n + \gamma_n x_n = \sum_m \kappa_{nm}, \quad (65)$$

$$\dot{\kappa}_{nm} = P_{nm} - K_{nm} \sin(x_n - x_m), \quad (66)$$

where $P_{nm} = -P_{mn}$, and $\sum_m P_{nm} = P_n$. This is inspired by Berner *et al.*,⁴³ but instead of the damping, we split the torque P_n and coupling $K_{nm} \sin(\cdot)$ into edge-wise contributions to allow for heterogeneous parameters in the stability conditions we obtain later. In the stationary, phase-locked state, all oscillators oscillate with a common frequency $\dot{x}_n^\circ = \Omega_{\text{sync}} = \sum_n P_n / \sum_n \gamma_n$ and satisfy the steady-state equations $P_{nm} = K_{nm} \sin(x_n^\circ - x_m^\circ)$. Again, we can assume $\sum_n P_n = 0$ without loss of generality. The κ_{nm}° correspond to the excess energy that flowed over the line in order to reach the steady state from an initial condition.

The system can be expressed as a system of coupled node variables $\mathbf{x} := (x_1, x_2, \dots, x_N)^\top$ and lexicographically ordered edge variables $\boldsymbol{\kappa} := (\kappa_1, \kappa_2, \dots, \kappa_L)^\top$ where each component κ_l corresponds to an edge $l = (n, m)$ with $n < m$. In this model, the antisymmetry $\kappa_{nm} = -\kappa_{mn}$ holds for the steady state and is conserved by the dynamics. This allows us to only consider edges with $n < m$. The N node and L edge variables are linked via an $N \times L$ signed incidence matrix \mathbf{B} , with all edges oriented from node n to node m . Denote $l = (l_1, l_2)$, then

$$B_{nl} = \delta_{nl_1} - \delta_{nl_2}. \quad (67)$$

In (65), we can use \mathbf{B} to sum over the edge variables, and in (66), we can use $\mathbf{B}^\top = \mathbf{B}^\dagger$ to obtain the phase differences. Introducing $\mathbf{M} := \text{diag}(m_1, m_2, \dots, m_N)$, $\boldsymbol{\Gamma} := \text{diag}(\gamma_1, \gamma_2, \dots, \gamma_N)$, $\mathbf{K} := \text{diag}(K_1, K_2, \dots, K_L)$, and $\mathbf{P} := (P_1, P_2, \dots, P_L)^\top$, the system is written as

$$\mathbf{M} \dot{\mathbf{x}} + \boldsymbol{\Gamma} \mathbf{x} = \mathbf{B} \boldsymbol{\kappa}, \quad (68)$$

$$\dot{\boldsymbol{\kappa}} = \mathbf{P} - \mathbf{K} \sin(\mathbf{B}^\top \mathbf{x}). \quad (69)$$

To linearize the system around the phase-locked state, we introduce error coordinates $\Delta \mathbf{x} = \mathbf{x} - \mathbf{x}^\circ$ and $\Delta \boldsymbol{\kappa} = \boldsymbol{\kappa} - \boldsymbol{\kappa}^\circ$. The linearized system reads

$$\mathbf{M} \Delta \dot{\mathbf{x}} + \boldsymbol{\Gamma} \Delta \mathbf{x} = \mathbf{B} \Delta \boldsymbol{\kappa}, \quad (70)$$

$$\Delta \dot{\boldsymbol{\kappa}} = -\mathbf{K} [\cos(\mathbf{B}^\top \mathbf{x}^\circ)] \mathbf{B}^\top \Delta \mathbf{x}. \quad (71)$$

In Laplace space, the transfer matrices of the system are

$$\Delta \mathbf{x} = \mathbf{T}^{ve}(s) \mathbf{B} \Delta \boldsymbol{\kappa}, \quad (72)$$

$$\mathbf{T}^{ve}(s) = \frac{1}{\mathbf{M}s + \boldsymbol{\Gamma}}, \quad (73)$$

$$\Delta \boldsymbol{\kappa} = -\mathbf{T}^{ev}(s) \mathbf{B}^\top \Delta \mathbf{x}, \quad (74)$$

$$\mathbf{T}^{ev}(s) = \frac{1}{s} \mathbf{K} [\cos \mathbf{B}^\top \mathbf{x}^\circ]. \quad (75)$$

With $\boldsymbol{\chi} = \mathbf{B} \boldsymbol{\kappa}$, we have

$$\Delta \mathbf{x} = \frac{1}{\mathbf{M}s + \boldsymbol{\Gamma}} \Delta \boldsymbol{\chi}, \quad (76)$$

$$\Delta \boldsymbol{\chi} = -\mathbf{B} \frac{1}{s} \mathbf{K} [\cos \mathbf{B}^\top \mathbf{x}^\circ] \mathbf{B}^\top \Delta \mathbf{x}, \quad (77)$$

and we can write the interconnected feedback loop as $\mathbf{T}^{ve} \# \mathbf{B} \mathbf{T}^{ev} \mathbf{B}^\top$.

To apply Proposition 5, we must ensure that \mathbf{T}^{ve} and \mathbf{T}^{ev} satisfy the conditions for (semi-)stability and (semi-)sectoriality. Moreover, the DC phase center of both transfer matrices is assumed to be 0 by convention. The diagonal matrices $\mathbf{T}^{ve} = \bigoplus_n \mathbf{T}_n^{ve}$ and $\mathbf{T}^{ev} = \bigoplus_l \mathbf{T}_l^{ev}$ have the entries

$$\mathbf{T}_n^{ve}(s) = \frac{1}{m_n s + \gamma_n}, \quad (78)$$

$$\mathbf{T}_l^{ev}(s) = \frac{1}{s} K_{nm} \cos(x_n^\circ - x_m^\circ). \quad (79)$$

For $\mathbf{T}^{ve}(s)$ to be stable, the poles at $s = -\frac{\gamma_n}{m_n}$ must lie in the left half of the complex plane, which requires $\frac{\gamma_n}{m_n} > 0$. Since the inertia $m_n > 0$, it follows that the damping must be positive: $\gamma_n > 0$. Then, it follows that the DC phase center $\mathbf{T}^{ve}(0)$ is 0 and that $\mathbf{T}^{ve}(s)$ is frequency-wise sectorial.

$\mathbf{T}^{ev}(s)$ is marginally stable (or semi-stable) because all poles lie on the imaginary axis at $s = 0$. Since $s = 0$ is a pole, the DC phase center is evaluated at $s = \epsilon^+$. For \mathbf{T}^{ev} to be frequency-wise semi-sectorial and full rank with a DC phase center of 0, $\mathbf{T}^{ev}(\epsilon^+)$ must be positive definite, which leads to the condition

$$\mathbf{T}_l^{ev}(\epsilon^+) = \frac{1}{\epsilon^+} K_{nm} \cos(x_n^\circ - x_m^\circ) > 0, \quad (80)$$

$$\implies |x_n^\circ - x_m^\circ| \begin{cases} < \frac{\pi}{2} & \text{if } K_{nm} > 0, \\ > \frac{\pi}{2} & \text{if } K_{nm} < 0 \end{cases} \quad (81)$$

for all links $l = (n, m)$.

Next, we evaluate the phase and gain conditions of Proposition 5. The phases of \mathbf{T}^{ve} range from 0 at $\omega = 0$ to $-\frac{\pi}{2}$ as $\omega \rightarrow \infty$, with $\phi(\mathbf{T}_n^{ve}(i\omega)) = -\arg(\gamma_n + im_n\omega)$ for all $\omega \in [0, \infty]$. The phases of \mathbf{T}^{ev} are constant over all $\omega \in [0, \infty] \setminus \Omega$, with $\phi(\mathbf{T}_l^{ev}(i\omega)) = -\frac{\pi}{2}$. With $\omega_c \in (0, \infty)$, the phase condition

$$\bar{\phi}(\mathbf{T}^{ve}(i\omega)) + \bar{\phi}(\mathbf{T}^{ev}(i\omega)) < \pi, \quad (82)$$

$$\underline{\phi}(\mathbf{T}^{ve}(i\omega)) + \underline{\phi}(\mathbf{T}^{ev}(i\omega)) > -\pi \quad (83)$$

is fulfilled for each $\omega \in [0, \omega_c) \setminus \Omega$.

T^{ve} and T^{ev} have the singular values

$$\sigma(T_n^{ve}(i\omega)) = \frac{1}{\sqrt{(m_n\omega)^2 + \gamma_n^2}}, \quad (84)$$

$$\sigma(T_l^{ev}(i\omega)) = \frac{1}{\omega} K_{nm} \cos(x_n^\circ - x_m^\circ), \quad (85)$$

where the gains $\bar{\sigma}(T^{ve}(i\omega))$ and $\bar{\sigma}(T^{ev}(i\omega))$ correspond to the largest singular values. With D being the maximum degree in the network, $\bar{\sigma}(\mathbf{B})^2$ is bounded from above by $2D$ [see (46) and (47)]. We can always find a cut-off frequency ω_c so that the gain condition

$$\bar{\sigma}(\mathbf{B})^2 \bar{\sigma}(T^{ve}) \bar{\sigma}(T^{ev}) \leq 2D \frac{K_{nm} \cos(x_n^\circ - x_m^\circ)}{\omega \sqrt{(m_n\omega)^2 + \gamma_n^2}} < 1 \quad (86)$$

is fulfilled for each $\omega \in [\omega_c, \infty)$.

These results show that we can apply Proposition 5 to prove stability for oscillators with $m_n > 0$, $\gamma_n > 0$, positive coupling $K_{nm} > 0$, and $|x_n^\circ - x_m^\circ| < \frac{\pi}{2}$ for connected (n, m) . For oscillators with negative coupling $K_{nm} < 0$, stability is ensured when the phase differences satisfy $|x_n^\circ - x_m^\circ| > \frac{\pi}{2}$ for connected (n, m) . This is the typical Laplacian formulation with Laplacian $\mathbf{L} = \mathbf{BK}[\cos \mathbf{B}^\top \mathbf{x}^\circ] \mathbf{B}^\top$, but we are allowed to leave out \mathbf{B} and \mathbf{B}^\top and only analyze the line weights.

C. An adaptive Kuramoto model

We study the adaptive Kuramoto model presented in Do et al.,²⁵ with the modification that c_{nm} can vary for each link. The system consists of N adaptively coupled phase oscillators,

$$\dot{x}_n = \psi_n - \sum_{m \neq n}^N A_{nm} \sin(x_n - x_m), \quad (87)$$

$$\dot{A}_{nm} = \cos(x_n - x_m) - c_{nm} A_{nm}, \quad (88)$$

where x_n denotes the phase and ψ_n the intrinsic frequency of node n . The coupling matrix $\mathbf{A} \in \mathbb{R}^{N \times N}$ defines an undirected, weighted network, where two oscillators (n, m) are connected if $A_{nm} = A_{mn} \neq 0$. The coupling is adaptive and co-evolves with the dynamics of the oscillators. In the stationary phase-locked state, all oscillators oscillate with a common frequency $\Psi = \frac{1}{N} \sum_n \psi_n$, which we can assume to be zero without loss of generality, and $A_{nm}^\circ = \cos(x_m^\circ - x_n^\circ)/c_{nm}$.

We now bring the system in the form of an input-output system with node variables $\mathbf{x} = (x_1, x_2, \dots, x_N)^\top$ and lexicographically ordered edge variables $\mathbf{a} = (a_1, a_2, \dots, a_L)^\top$, where each component a_l corresponds to an edge $l = (n, m)$ with $n < m$. The corresponding outputs of the node and edge dynamics are \mathbf{o} and \mathbf{u} , respectively. The N nodes and L edges are linked via the $N \times L$ incidence matrix \mathbf{B} , where we assume that each edge is oriented from node n to node m . Introducing $\mathbf{C} = \text{diag}(c_1, c_2, \dots, c_L)$, the system is written as

$$\dot{\mathbf{x}} = \boldsymbol{\psi} + \mathbf{u}, \quad (89)$$

$$\mathbf{o} = \mathbf{x}, \quad (90)$$

$$\dot{\mathbf{a}} = \cos(\mathbf{B}^\top \mathbf{o}) - \mathbf{C}\mathbf{a}, \quad (91)$$

$$\mathbf{u} = -\mathbf{B}(\mathbf{a} \circ \sin(\mathbf{B}^\top \mathbf{o})), \quad (92)$$

where \circ denotes element-wise multiplication.

To linearize the system around the phase-locked state, we introduce error coordinates $\Delta \mathbf{x} = \mathbf{x} - \mathbf{x}^\circ$, $\Delta \mathbf{o} = \mathbf{o} - \mathbf{o}^\circ$, $\Delta \mathbf{a} = \mathbf{a} - \mathbf{a}^\circ$, and $\Delta \mathbf{u} = \mathbf{u} - \mathbf{u}^\circ$, where $\dot{\mathbf{x}}^\circ = \Psi$ and $\mathbf{a}^\circ = \mathbf{C}^{-1} \cos(\mathbf{B}^\top \mathbf{x}^\circ)$. The linearized system reads

$$\Delta \dot{\mathbf{x}} = \Delta \mathbf{u}, \quad (93)$$

$$\Delta \dot{\mathbf{o}} = \Delta \mathbf{x}, \quad (94)$$

$$\Delta \dot{\mathbf{a}} = -\mathbf{C}\Delta \mathbf{a} - [\sin(\mathbf{B}^\top \mathbf{x}^\circ)] \mathbf{B}^\top \Delta \mathbf{o}, \quad (95)$$

$$\Delta \mathbf{u} = -\mathbf{B}([\sin(\mathbf{B}^\top \mathbf{x}^\circ)] \Delta \mathbf{a} + \mathbf{C}^{-1}[\cos^2(\mathbf{B}^\top \mathbf{x}^\circ)] \mathbf{B}^\top \Delta \mathbf{o}). \quad (96)$$

To simplify the analysis, we introduce $\Delta \mathbf{v} = \frac{1}{s} \Delta \mathbf{u}$. In Laplace space, the transfer matrices of the system are

$$\Delta \mathbf{o} = T^{ve}(s) \Delta \mathbf{v}, \quad (97)$$

$$T^{ev}(s) = \mathbf{I}, \quad (98)$$

$$\Delta \mathbf{v} = -\mathbf{B}T^{ev}(s)\mathbf{B}^\top \Delta \mathbf{o}, \quad (99)$$

$$T^{ev}(s) = (s\mathbf{C})^{-1}[\cos^2(\mathbf{B}^\top \mathbf{x}^\circ)] - (s(\mathbf{I} + \mathbf{C}))^{-1}[\sin^2(\mathbf{B}^\top \mathbf{x}^\circ)]. \quad (100)$$

To apply phase and gain conditions, we must ensure that the transfer matrices satisfy the conditions for (semi-)stability, (semi-)sectoriality, and the DC phase center. $T^{ve} = \mathbf{I}$ is stable and frequency-wise sectorial with a DC phase center of $T^{ve}(0) = 0$. The diagonal matrix $T^{ev} = \bigoplus_l T^{ev}_l$ has the entries

$$T_l^{ev}(s) = \frac{1}{s c_{nm}} \cos^2(x_n^\circ - x_m^\circ) - \frac{1}{s(s + c_{nm})} \sin^2(x_n^\circ - x_m^\circ). \quad (101)$$

$T^{ev}(s)$ has poles at $s = 0$ and at $s = -c_{nm}$, which requires $c_{nm} \geq 0$ for semi-stability and $c_{nm} \neq 0$ for boundedness. For T^{ev} to be frequency-wise semi-sectorial and have a full rank along the indented imaginary axis with a DC phase center of 0, $T^{ev}(\epsilon^+)$ must be positive definite, which leads to the condition

$$\frac{1}{c_{nm}} \cos^2(x_n^\circ - x_m^\circ) - \frac{1}{\epsilon^+ + c_{nm}} \sin^2(x_n^\circ - x_m^\circ) > 0. \quad (102)$$

This must hold for arbitrarily small ϵ^+ ; thus,

$$\frac{1}{c_{nm}} \cos^2(x_n^\circ - x_m^\circ) - \frac{1}{c_{nm}} \sin^2(x_n^\circ - x_m^\circ) > 0 \quad (103)$$

$$\implies \cos(2(x_n^\circ - x_m^\circ)) > 0 \quad (104)$$

$$\implies |x_n^\circ - x_m^\circ| > \frac{\pi}{4}. \quad (105)$$

Next, we analyze the interconnected system $T^{ve} \# \mathbf{B}T^{ev}\mathbf{B}^\top$ and evaluate the phase and gain conditions.

T^{ve} has phase $\phi(T^{ve}(i\omega)) = 0$ for all s . The phases of T^{ev} lie in $[0, \phi_c] - \frac{\pi}{2}$ for $\omega \in [0, \infty) \setminus \Omega$, with $\phi_c \in [\arctan \frac{1}{2}, \frac{\pi}{4}]$ depending on the phase differences,

$$\phi_c := \max_{l=(n,m)} \arctan \left\{ \left[2 \cos^2(x_n^\circ - x_m^\circ) \right]^{-1} \right\}. \quad (106)$$

Hence, the phase condition

$$\bar{\phi}(T^{ve}(i\omega)) + \bar{\phi}(T^{ev}(i\omega)) < \pi, \quad (107)$$

$$\phi(T^{ve}(i\omega)) + \phi(T^{ev}(i\omega)) > -\pi \quad (108)$$

is fulfilled for each $\omega \in [0, \infty) \setminus \Omega$. We, therefore, do not need the gain condition and can apply Theorem 4 to prove stability for $c_{nm} > 0$ and oscillators satisfying $|x_n^\circ - x_m^\circ| < \frac{\pi}{4}$ for all edges. This agrees with the necessary stability conditions presented in Do *et al.*²⁵ for the case of homogeneous parameters, showing that the condition is exact in this setting. Thus, the combined results completely settle the linear stability of this adaptive Kuramoto model.

VI. DISCUSSION

This paper introduced a new method for studying the linear stability of steady states in adaptive networks. By leveraging new results from linear algebra and control theory, we could give novel, local stability conditions. Applying these to the classical Kuramoto model and the Kuramoto model with inertia (written as adaptive first-order oscillators) demonstrated that they are not overly conservative and allow straightforward generalization to heterogeneous parameters. In the case of truly adaptive oscillators, the sufficient conditions we obtain even match necessary conditions derived previously. However, our conditions apply much more broadly, including the case of heterogeneous parameters as well. This gives a complete characterization of the stability of steady states of this adaptive Kuramoto model in situations in which the necessary result applies.

One notable aspect of the theory developed here is that the stability conditions are fully local, and nodes and edges are allowed to be highly heterogeneous in their states and dynamics. Contrary to work in the master stability tradition, we do not require any factorization of the system's Jacobian of the type $J = F \otimes I + G \otimes L$ with homogeneous local dynamics F and coupling G . This could be particularly important for the study of multilayer networks with different topologies in the different layers, where no such factorization is available.

The natural way in which phase conditions and network structures interact also allows many further generalizations of the above framework. Due to the fact that edge states have their own full dynamics, there is considerable freedom in choosing exactly how the system is partitioned into edges and nodes. The structured perturbation approach of Woolcock and Schmid³⁵ is an example of this.

There also are further variations of phase-based stability conditions that could be interesting to study, particularly for directed networks. Notions, such as r -sectoriality, can combine gain and phase information in ways that encode directedness in a natural way.²²

Finally, the examples explored above used a signed incidence matrix and, thus, Laplacian-type diffusive coupling. However, the

theorem leaves the nature of B completely open. We leave exploring the use of this theorem for systems where the coupling is not Laplacian in nature, e.g., additive, to future work.

ACKNOWLEDGMENTS

This work was supported by the OpPoDyn Project, Federal Ministry for Economic Affairs and Climate Action (No. FKZ:03EI1071A). J.N. gratefully acknowledges support by BIMoS (TU Berlin), Studienstiftung des Deutschen Volkes, and the Berlin Mathematical School, funded by the Deutsche Forschungsgemeinschaft (DFG, German Research Foundation) Germany's Excellence Strategy—The Berlin Mathematics Research Center MATH+ (EXC-2046/1, Project ID: 390685689). R.D. was supported by the Swiss National Science Foundation under Grant No. 200021_215336.

AUTHOR DECLARATIONS

Conflict of Interest

The authors have no conflicts to disclose.

Author Contributions

Nina Kastendiek and Jakob Niehues contributed equally to this paper.

Nina Kastendiek: Formal analysis (equal); Investigation (equal); Methodology (supporting); Visualization (lead); Writing – original draft (equal); Writing – review & editing (equal). **Jakob Niehues:** Conceptualization (equal); Formal analysis (equal); Investigation (equal); Methodology (equal); Supervision (equal); Writing – original draft (equal); Writing – review & editing (equal). **Robin Delabays:** Conceptualization (equal); Methodology (equal); Writing – review & editing (supporting). **Thilo Gross:** Conceptualization (supporting); Supervision (supporting); Writing – original draft (supporting); Writing – review & editing (equal). **Frank Hellmann:** Conceptualization (equal); Methodology (equal); Supervision (equal); Writing – original draft (equal); Writing – review & editing (equal).

DATA AVAILABILITY

The data that support the findings of this study are available within the article.

APPENDIX: CONSTANT RANK LEMMA

Lemma 6: Let $M_1(s), \dots, M_N(s)$ be a set of matrix valued functions. Assume that for any s , all the $M_i(s)$ are semi-sectorial, have full rank, and their maximum and minimum phases satisfy

$$\max_i \bar{\phi}(M_i(s)) - \min_i \underline{\phi}(M_i(s)) < \pi, \quad (A1)$$

then

$$\ker \left(B \bigoplus_i M_i(s) B^\dagger \right) = \ker(B^\dagger). \quad (A2)$$

In particular, the matrix $B \bigoplus_i M_i(s) B^\dagger$ has constant rank as a function of s .

Proof. For semi-sectorial matrices satisfying the minimum-maximum angle condition above, 0 can only be on a corner of the numerical range and, thus, has to be an eigenvalue. Thus, for such matrices, being full rank implies sectoriality and 0 cannot be in their numerical range. Furthermore, the numerical ranges of $W(M_i)$ at fixed s lie in the same open half plane.

Let us define $M(s) := \bigoplus_i M_i(s)$. First, it is clear that $\ker(BM(s)B^\dagger) \subset \ker(B^\dagger)$. Indeed, if $B^\dagger z = 0$, then $BM(s)B^\dagger z = 0$.

Second, let $z \notin \ker(B^\dagger)$, i.e., $B^\dagger z \neq 0$. From the assumption that all $M_i(s)$ have their numerical ranges in the same open half-plane, it follows that $M(s)$ has full rank and then $M(s)B^\dagger z \neq 0$. Furthermore, by the convex hull property, the numerical range of $M(s)$ lies in an open half-plane, and therefore,

$$z^\dagger BM(s)B^\dagger z \neq 0, \quad (A3)$$

meaning that $BM(s)B^\dagger z$ cannot be zero. Hence, z does not belong to the kernel of $BM(s)B^\dagger$, which concludes the proof of Eq. (A2).

Finally, as neither B nor its kernel depends on s , the kernel is constant with respect to s . \square

REFERENCES

- ¹T. Gross and B. Blasius, "Adaptive coevolutionary networks: A review," *J. R. Soc. Interface* **5**, 259–271 (2008).
- ²T. Gross, C. J. Dommar D'Lima, and B. Blasius, "Epidemic dynamics on an adaptive network," *Phys. Rev. Lett.* **96**, 208701 (2006).
- ³V. Marceau, P.-A. Noël, L. Hébert-Dufresne, A. Allard, and L. J. Dubé, "Adaptive networks: Coevolution of disease and topology," *Phys. Rev. E* **82**, 036116 (2010).
- ⁴S. V. Scarpino, A. Allard, and L. Hébert-Dufresne, "The effect of a prudent adaptive behaviour on disease transmission," *Nat. Phys.* **12**, 1042–1046 (2016).
- ⁵B. Kozma and A. Barrat, "Consensus formation on adaptive networks," *Phys. Rev. E* **77**, 016102 (2008).
- ⁶H. Rainer and U. Krause, "Opinion dynamics and bounded confidence: Models, analysis and simulation," *J. Artif. Soc. Soc. Simul.* **5**, 1–12 (2002).
- ⁷F. Vazquez, V. M. Eguíluz, and M. S. Miguel, "Generic absorbing transition in coevolution dynamics," *Phys. Rev. Lett.* **100**, 108702 (2008).
- ⁸I. D. Couzin, C. C. Ioannou, G. Demirel, T. Gross, C. J. Torney, A. Hartnett, L. Conrad, S. A. Levin, and N. E. Leonard, "Uninformed individuals promote democratic consensus in animal groups," *Science* **334**, 1578–1580 (2011).
- ⁹B. Skyrms and R. Pemantle, "A dynamic model of social network formation," in *Adaptive Networks: Theory, Models and Applications* (Springer, 2009), pp. 231–251.
- ¹⁰A.-L. Do, L. Rudolf, and T. Gross, "Patterns of cooperation: Fairness and coordination in networks of interacting agents," *New J. Phys.* **12**, 063023 (2010).
- ¹¹S. Bornholdt and T. Rohlf, "Topological evolution of dynamical networks: Global criticality from local dynamics," *Phys. Rev. Lett.* **84**, 6114 (2000).
- ¹²C. Meisel and T. Gross, "Adaptive self-organization in a realistic neural network model," *Phys. Rev. E* **80**, 061917 (2009).
- ¹³C. Kuehn, "Time-scale and noise optimality in self-organized critical adaptive networks," *Phys. Rev. E* **85**, 026103 (2012).
- ¹⁴R. L. G. Raimundo, P. R. Guimarães, and D. M. Evans, "Adaptive networks for restoration ecology," *Trends Ecol. Evol.* **33**, 664–675 (2018).
- ¹⁵R. Berner, T. Gross, C. Kuehn, J. Kurths, and S. Yanchuk, "Adaptive dynamical networks," *Phys. Rep.* **1031**, 1–59 (2023).
- ¹⁶G. Demirel, F. Vazquez, G. A. Böhme, and T. Gross, "Moment-closure approximations for discrete adaptive networks," *Phys. D* **267**, 68–80 (2014).
- ¹⁷L. A. Segel and S. A. Levin, "Application of nonlinear stability theory to the study of the effects of diffusion on predator-prey interactions," *AIP Conf. Proc.* **27**, 123–152 (1976). "Application of nonlinear stability theory to the study of the effects of diffusion on predator-prey interactions," in *AIP Conference Proceedings* (American Institute of Physics, 1976), Vol. 27, pp. 123–152, see <https://www.jasss.org/5/3/2.html>
- ¹⁸L. M. Pecora and T. L. Carroll, "Master stability functions for synchronized coupled systems," *Phys. Rev. Lett.* **80**, 2109 (1998).
- ¹⁹R. Berner, S. Vock, E. Schöll, and S. Yanchuk, "Desynchronization transitions in adaptive networks," *Phys. Rev. Lett.* **126**, 028301 (2021).
- ²⁰R. Berner and S. Yanchuk, "Synchronization in networks with heterogeneous adaptation rules and applications to distance-dependent synaptic plasticity," *Front. Appl. Math. Stat.* **7**, 714978 (2021).
- ²¹D. Wang, W. Chen, S. Z. Khong, and L. Qiu, "On the phases of a complex matrix," *Linear Algebra Appl.* **593**, 152–179 (2020).
- ²²D. Wang, X. Mao, W. Chen, and L. Qiu, "On the phases of a semi-sectorial matrix and the essential phase of a Laplacian," *Linear Algebra Appl.* **676**, 441–458 (2023).
- ²³W. Chen, D. Wang, S. Z. Khong, and L. Qiu, "A phase theory of multi-input multi-output linear time-invariant systems," *SIAM J. Control Optim.* **62**, 1235–1260 (2024).
- ²⁴D. Zhao, W. Chen, and L. Qiu, "When small gain meets small phase," *arXiv:2201.06041* (2022).
- ²⁵A. L. Do, S. Boccaletti, J. Epperlein, S. Siegmund, and T. Gross, "Topological stability criteria for networking dynamical systems with Hermitian Jacobian," *Eur. J. Appl. Math.* **27**, 888–903 (2016).
- ²⁶J. Niehues, R. Delabays, and F. Hellmann, "Small-signal stability of power systems with voltage droop," *arXiv:2411.10832* (2024).
- ²⁷R. Kogler, A. Plietzsch, P. Schultz, and F. Hellmann, "Normal form for grid-forming power grid actors," *PRX Energy* **1**, 013008 (2022).
- ²⁸A. Büttner and F. Hellmann, "Complex couplings—A universal, adaptive, and bilinear formulation of power grid dynamics," *PRX Energy* **3**, 013005 (2024).
- ²⁹G. Zames, "On the input-output stability of time-varying nonlinear feedback systems Part one: Conditions derived using concepts of loop gain, conicity, and positivity," *IEEE Trans. Autom. Control* **11**, 228–238 (1966).
- ³⁰Y. Kuramoto, *Self-entrainment of a Population of Coupled Non-linear Oscillators* (Springer, 1975), pp. 420–422.
- ³¹W. S. Levine, *The Control Systems Handbook: Control System Advanced Methods* (CRC Press, 2018).
- ³²J. Bechhoefer, *Control Theory for Physicists*, 1st ed. (Cambridge University Press, 2021).
- ³³The term DC means "direct current" and refers to evaluation at zero frequency.
- ³⁴K. Zhou, *Essentials of Robust Control* (Prentice Hall, 1998).
- ³⁵L. Woolcock and R. Schmid, "Mixed gain/phase robustness criterion for structured perturbations with an application to power system stability," *IEEE Control Syst. Lett.* **7**, 3193–3198 (2023).
- ³⁶From here on, we use the same letter for the Laplace transform of a quantity, following convention.
- ³⁷R. A. Horn and C. R. Johnson, *Matrix Analysis*, 2nd ed. (Cambridge University Press, 2012).
- ³⁸To see this, consider the stacked system of complexified x and the complex conjugate x^* , which is unitarily equivalent to a real system of stacked $\Re x$ and $\Im x$.
- ³⁹M. Thümler, S. G. Srinivas, M. Schröder, and M. Timme, "Synchrony for weak coupling in the complexified Kuramoto model," *Phys. Rev. Lett.* **130**, 187201 (2023).
- ⁴⁰S. Lee, L. Braun, F. Bönisch, M. Schröder, M. Thümler, and M. Timme, "Complexified synchrony," *Chaos* **34**, 053141 (2024).
- ⁴¹A. Bergen and D. Hill, "A structure preserving model for power system stability analysis," *IEEE Trans. Power Appar. Syst.* **PAS-100**, 25–35 (1981).
- ⁴²G. Filatrella, A. H. Nielsen, and N. F. Pedersen, "Analysis of a power grid using a Kuramoto-like model," *Eur. Phys. J. B* **61**, 485–491 (2008).
- ⁴³R. Berner, S. Yanchuk, and E. Schöll, "What adaptive neuronal networks teach us about power grids," *Phys. Rev. E* **103**, 042315 (2021).